Cardiovascular protective effects of nebivolol in Zucker diabetic fatty rats

Jorge E. Toblli[a], Gabriel Cao[a], Carlos Rivas[a], Marina Munoz[b], Jorge Giani[b], Fernando Dominici[b] and Margarita Angerosa[a]

Background **Although effective in reducing blood pressure, therapy with a first-generation β-blocker is currently controversial in metabolic syndrome due to its negative impact on carbohydrate and lipid metabolism.**

Objective and design **We evaluated the effects of nebivolol, a third-generation highly selective β-blocker with additional vasodilating activity, versus the traditional β-blocker atenolol in controlling functional and morphological cardiovascular damage in a rat model of metabolic syndrome.**

Methods **During 6 months, Zucker diabetic fatty (ZDF) rats and control lean Zucker rats (LZR) were studied. The experimental groups were: untreated ZDF, ZDF along with nebivolol, ZDF along with atenolol and LZR. Blood pressure, plasma insulin, triglycerides, cholesterol, glucose and platelet aggregation were evaluated. Malondialdehyde, reduced glutathione (GSH)/oxidized glutathione (GSSG) ratio, CuZn superoxide dismutase, catalase and glutathione peroxidase were determined in heart homogenates and transforming growth factor β_1 and plasminogen activator inhibitor-1 (PAI-1) expression, by immunohistochemistry (IHC). Vascular reactivity, vascular cell adhesion molecule-1, platelet endothelial cell adhesion molecule-1, PAI-1, enhanced nitric oxide synthase and collagen expression were evaluated in aorta.**

Results **Nebivolol and atenolol presented a similar reduction in blood pressure. However, nebivolol showed a better lipid profile, preserved left ventricular function, a significant control in left ventricular geometry and moderated left ventricular hypertrophy versus atenolol. Significant reduction in platelet aggregation and a substantial endothelium-dependent and endothelium-independent relaxation in vessels were also shown in the nebivolol group versus atenolol group. Antioxidant defenses were preserved by nebivolol with a reduction in oxidative stress parameters. Vascular cell adhesion molecule-1, platelet endothelial cell adhesion molecule-1, PAI-1 and eNOS were favorably modulated with nebivolol in vessel wall. TGFβ_1, PAI-1 and accumulation of collagen-III and collagen-I were also diminished in heart with nebivolol.**

Conclusion **The present study provides substantial information supporting an actual protective role of nebivolol in comparison with atenolol in experimental metabolic syndrome. *J Hypertens* 28:1007–1019 © 2010 Wolters Kluwer Health | Lippincott Williams & Wilkins.**

Journal of Hypertension 2010, **28**:1007–1019

Keywords: aorta, beta-blockers, heart, metabolic syndrome, Zucker diabetic fatty rat

Abbreviations: CuZnSOD, CuZn superoxide dismutase; GPx, glutathione peroxidase; GSH, reduced glutathione; LVDD, left ventricle end-diastolic diameter; LVM, left ventricular mass; LVPW, left ventricular posterior wall in diastole; LVSD, left ventricle end-systolic diameter; LZR, lean Zucker rats; NIDDM, diabetes mellitus; PAI-1, plasminogen activator inhibitor-1; PECAM-1, platelet endothelial cell adhesion molecule-1; TBARS, thiobarbituric acid reactive species; VCAM-1, vascular cell adhesion molecule-1; ZDF, Zucker diabetic fatty rats

[a]Laboratory of Experimental Medicine, Hospital Alemán and [b]IQUIFIB. School of Pharmacy and Biochemistry. University of Buenos Aires, Buenos Aires, Argentina

Correspondence to Jorge E. Toblli, MD, PhD, FASN, Laboratory of Experimental Medicine, Hospital Alemán, Av. Pueyrredón 1640, Buenos Aires 1118, Argentina
Tel: +54 11 4827 7000; fax: +54 11 4805 6087;
e-mail: jorgetoblli@fibertel.com.ar

Received 10 August 2009 **Revised** 2 January 2010
Accepted 8 January 2010

Introduction

The association of obesity, type 2 diabetes and arterial hypertension is increasing in prevalence, nowadays affecting a large population worldwide. Furthermore, when together, they constitute a metabolic syndrome, which is deeply involved in the development of cardiovascular disease, with deleterious consequences [1–5]. The sympathetic nervous system is an important regulatory mechanism of both metabolic and cardiovascular disease function, and altered sympathetic activity may play a role in the cause and/or complications of metabolic syndrome. At present, it remains unresolved whether aberrations of the sympathetic nervous system contribute to metabolic syndrome or are rather a consequence of it. The possibility that a primary increase in sympathetic tone might contribute to the development of obesity and metabolic syndrome is supported by longitudinal data in Japanese men. Masuo *et al.* [6] reported that elevated plasma norepinephrine levels at baseline predicted future higher blood pressure (BP) readings, gain of weight and higher insulin values over a 5-year follow-up. Several components of the metabolic syndrome may enhance sympathetic drive. Hyperinsulinemia, the hallmark of reduced insulin sensitivity, can directly stimulate

0263-6352 © 2010 Wolters Kluwer Health | Lippincott Williams & Wilkins DOI:10.1097/HJH.0b013e328337598c

sympathetic nervous system activity in human beings [7]. Products of adipose tissue, such as leptin and nonesterified fatty acids, may also contribute to neurogenic activation and insulin resistance in persons with abdominal obesity [8,9].

β-adrenergic receptor antagonists are effective for the treatment of hypertension, but they are underused in diabetic patients because of possible adverse effects on carbohydrate and lipid metabolism, including insulin resistance, glucose intolerance and dyslipidemia. Traditional β-blockers, both nonselective and selective, are vasoconstrictive due to unopposed α1 activity; however, vasodilating β-blockers, such as nebivolol, are not associated with these negative metabolic effects.

The Zucker diabetic fatty (ZDF) rat is a recognized model of obesity, type 2 diabetes, arterial hypertension and hyperlipidemia [10–12]. Thus, it is an attractive experimental model to investigate cardiovascular damage related to the human 'metabolic syndrome'.

According to this background, the purpose of the present long-term study is to evaluate whether nebivolol is more effective than the traditional β-blocker atenolol in controlling functional as well as morphological cardiovascular damage in this representative rat model of human metabolic syndrome. On this regard, using different laboratory techniques, carbohydrate and lipid metabolism, vascular reactivity, platelet aggregation, oxidative stress, inflammatory/fibrosis-related molecules' expression in tissue, as well as echocardiographic and BP parameters were assessed.

Methods

Animals and treatments

Twelve-weeks-old male ZDF rats and control lean Zucker rat (LZR) (Charles River Laboratories, Wilmington, Massachusetts, USA) were housed in individual cages at $21 \pm 2^{\circ}C$ and a 12-h light/darkness cycle (0700 to 1900 h), and divided into four groups: ZDF group (G1, $n = 8$); ZDF with nebivolol group (G2, $n = 8$); ZDF with atenolol group (G3, $n = 8$); and LZR group (G4, $n = 8$). All the animals received tap water standard rat chow (18–20%) '*ad libitum*'. During 6 months, all the rats were treated according to the following schedule: G1, receiving no treatment; G2, receiving nebivolol (10 mg/kg per day) [13]; G3, receiving atenolol (100 mg/kg per day) [14]; and G4, receiving no treatment. Nebivolol and atenolol were administered in drinking water, and dose treatment was adjusted each week on the basis of the calculation of the body weight for each animal. Biochemical determinations were assessed at baseline and at the end of the experiment. After 6 months of treatment, all the rats were euthanized by subtotal exsanguinations under anesthesia [sodium thiopental 40 mg/kg, intraperitoneal (i.p.)]. The heart and aorta were rapidly excised, weighed and harvested for oxidative stress evaluation, light microscopy and immunohistochemistry (IHC) and 'in-vitro' studies.

Blood pressure measurement

SBP was measured monthly from baseline to the end of the experiment by tail-cuff plethysmography, as previously described [13,14].

Biochemical procedures

After 14 h fasting, rat blood samples were collected from the tail vein in capillary tubes at baseline, and at the end of the experiment, from the inferior cava vein before the rats were being sacrificed. Plasma glucose level was measured by the glucose oxidase method with an automatic analyzer (Hitachi 911; Hitachi, Tokyo, Japan). Serum cholesterol and triglycerides were assessed according to standard methods. Serum insulin was determined by sensitive rat insulin RIA kit (SRI-13; LINCO Research, St. Charles, Missouri, USA). Serum samples were stored prior to testing. Serum electrolytes were determined by standard methods.

Platelet aggregation response

Evaluation of platelet aggregation was assessed by citrated plasma enrichment in platelets (PEP) samples obtained from whole blood in 3.8% sodium citrate centrifuged at 200 rpm during 10 min [15]. Then, PEP was separated into another tube, avoiding red blood cell contamination. These tubes were conserved and covered until their process. The rest of the blood samples were centrifuged at 3000 rpm during 30 min in order to obtain plasma poor in platelets (PPP). All samples were analyzed within 2 h from the collection time. Evaluation of platelet aggregation was performed using a double-channel aggregometer (Chrono-log Corporation, Havertown, Pennsylvania, USA). This equipment continuously records changes in optic density of PEP after addition of an agonist or inductor. For this purpose, the potential influence of several parameters was investigated, using ADP, arachidonic acid, collagen and collagen with epinephrine. The extent of aggregation was estimated by the percentage of maximum increase in light transmission, with the buffer representing 100% transmittance.

Oxidative stress parameters' evaluation in heart

Homogenates preparation

A fraction of heart was homogenized (1 : 3, weight : volume) in ice-cold 0.25 mol/l sucrose. Reduced glutathione (GSH) levels were determined in the 10 000*g* supernatant following methods as previously described [16–19]. Another fraction of each corresponding perfused tissue was homogenized (1 : 10, weight : volume) in 0.05 mol/l sodium phosphate buffer, pH 7.4, and was directly used for the determination of malondialdehyde in order to evaluate lipoperoxidation by thiobarbituric acid-reactive species or it was centrifuged at 4°C during 15 min at 9500*g*. The resulting supernatant was used for

measuring catalase activity. Finally, another fraction of each corresponding perfused tissue fraction was homogenized (1 : 3, weight : volume) in ice-cold sucrose (0.25 mol/l). The supernatant obtained after centrifugation at 105 000*g* for 90 min was used for measuring CuZn superoxide dismutase (CuZnSOD) and glutathione peroxidase (GPx) activity.

Echocardiographic evaluation of the left ventricle

Transthoracic echocardiograms were obtained from each rat, without anesthesia, using a Toshiba echocardiographic system (Toshiba, Tokyo, Japan) with a 7.5-MHz transducer at baseline and at the end of the experiment [20]. M-mode and bidimensional echocardiography was performed in minor axis, at the level of papillary muscle. The thickness of the interventricular septum (IVS) and the left ventricular posterior wall in diastole (LVPW) were determined in the parasternal long axis at the midchordal level. Left ventricular dimensions, left ventricle end-diastolic diameter (LVDD) and left ventricle end-systolic diameter (LVSD), were measured perpendicularly to the long axis of the ventricle at the midchordal level. Fractional shortening was calculated as the end-systolic dimension subtracted from the end-diastolic dimension and divided by the end-diastolic dimension. Left ventricular mass (LVM) was determined using the standard cube method.

Organ bath studies (*in vitro*)

The thoracic aorta artery was removed and immediately dissected [12,21]. Aortic rings (10-mm diameter) were then transferred to ice-cold Krebs-bicarbonate solution. The aortic rings were mounted on a vertical organ bath system (MyoBath-4; World Precision Instrument, Inc., Sarasota, Florida, USA), using chambers containing 5-ml Krebs-bicarbonate solution. The tissue was connected to a force–displacement transducer (FORT10; World Precision Instrument, Inc.). A pretension of 1000 mg (optimal tension defined in preliminary experiments) was applied, and the rings were allowed to equilibrate for 45–60 min without additional mechanical manipulation. During the equilibration, the organ bath solution was replaced every 15 min. At the end of the equilibration period, a concentration–response curve to phenylephrine (Phe, 10–8 to 10–4 mol/l) was performed for each sample. Next, in order to explore endothelium-dependent vasorelaxation, a concentration–response curve to acetylcholine (ACh, 10–8 to 10–4 mol/l) was conducted on the Phe-induced (10–4 mol/l) aortic rings. Finally, responses of Phe-induced precontracted aorta rings to cumulative additions of sodium nitroprusside (SNP, 10–8 to 10–4 mol/l) were studied with the purpose of exploring endothelium-independent vasorelaxation. The contractile responses were expressed as the absolute change in maximal developed tension (mg), normalized per milligram tissue weight and the relaxation, as the percentage of changes in Phe-induced tone. Concentration inducing 50% of maximal effect was expressed as pD2.

Heart and aorta histology, processing and examination

The heart and aorta were perfused with saline solution through the abdominal aorta until they were free of blood. Tissue was fixed in phosphate-buffered 10% formaldehyde (pH 7.2) and embedded in paraffin. Three-micron sections were cut and stained with hematoxilin–eosin (H&E) and Masson's trichrome. All observations in light microscopy were performed using a light microscope, Nikon E400 (Nikon Instrument Group, Melville, New York, USA).

Immunohistochemical staining

mAbs against transforming growth factor β_1 (TGFβ_1) (Santa Cruz Biotechnology, Inc., Santa Cruz, California, USA) at a dilution of 1 : 100 and anticollagen type I and type III (Biogenex, San Roman, California, USA) at a dilution of 1 : 100 were used to evaluate the process of fibrosis. Plasminogen activator inhibitor-1 (PAI-1) in heart and aorta, a rabbit polyclonal antirat immunoglobulin G (IgG) anti-PAI-1 (American Diagnostica, Greenwich, Connecticut, USA), at a dilution of 1 : 100 was used. The cell adhesion molecules, vascular cell adhesion molecule-1 (VCAM-1) and platelet endothelial cell adhesion molecule-1 (PECAM-1), were also evaluated in aorta. A rabbit polyclonal anti-VCAM-1 (sc-8304; Santa Cruz Biotechnology, Inc.) at a dilution of 1 : 100 and a goat polyclonal anti-PECAM-1 (sc-1506; Santa Cruz Biotechnology, Inc.) at a dilution of 1 : 100 were used. Immunostaining was carried out with a commercially modified avidin–biotin–peroxidase complex technique and counterstained with hematoxilin.

Morphological analysis

All tissue samples were evaluated independently by two investigators without prior knowledge of the group to which the rats belonged. All measurements were carried out using an image analyzer, Image-Pro Plus version 4.5 for windows (Media Cybernetics, LP, Silver Spring, Maryland, USA). Histomorphometric evaluation of heart was carried out according to the following schedule: extracellular matrix expansion (ECM), and wall/lumen ratio in heart vessels within the confines of each of the 20 random 1.13 mm^2 adjacent fields, viewed at 400× magnification. In every heart, positive immunostaining for PAI-1, TGFβ_1, collagen I and III was assessed. In aorta, positive immunostaining for VCAM-1, PECAM-1, PAI-1, TGFβ_1, and collagen III was evaluated.

Immunoprecipitation and immunoblotting

Aorta samples were homogenized in 10 volumes of a solubilization buffer containing 1% Triton X-100 Sigma Ultra (Sigma, St. Louis, Missouri, USA), together with protease inhibitors, as previously described [22,23]. To determine the protein level of PECAM-1, VCAM-1, PAI-1

and enhanced nitric oxide synthase (eNOS) in aorta, equal amounts of solubilized proteins (80 μg) were denatured by being boiled in reducing sample buffer and resolved by SDS-PAGE. Western transfer of proteins to polyvinylidene difluoride membranes was performed, as previously described [23]. The membranes were then incubated overnight with the following antibodies: anti-PECAM-1 (sc-1506), anti-VCAM-1 (sc-8304), anti-PAI-1 (sc-8979) or anti-eNOS (sc-654) (1 : 1000 dilution for all antibodies). Membranes were then blocked by incubation for 2 h with a blocking buffer composed of Tris-buffered saline-Tween 20 (TBS-T) [10 mmol/l Tris HCl (pH 7.6), 150 mmol/l NaCl and 0.02% Tween 20 containing 3% BSA] and were finally incubated for 1 h with goat antirabbit IgG-horse radish peroxidase (HRP) secondary antibody (for VCAM-1, PAI-1 and eNOS) or goat antigoat IgG-HRP (for PECAM-1). Specific bands were detected by enhanced chemiluminescence (ECL; Amersham, Piscataway, New Jersey, USA), and their intensities were quantitated by digital densitometry.

Statistical method

Values were expressed as mean ± SD. All statistical analyses were performed using absolute values and processed through GraphPad Prism, version 5.0 (GraphPad Software, Inc. San Diego, California, USA). The assumption test to determine the Gaussian distribution was performed by the Kolmogorov–Smirnov method. For parameters with Gaussian distribution, comparisons among groups were carried out using one-way analysis of variance (ANOVA) followed by the Bonferroni's test, as well as two-way ANOVA for repeated measures, and Kruskal–Wallis test (nonparametric ANOVA) and Dunn's multiple comparison test were used when appropriated. A P value of less than 0.05 was considered significant.

Results

Blood pressure recordings

No differences were observed at baseline in all groups. On the contrary, untreated ZDF rats presented high BP throughout the study when compared with LZR (Fig. 1a. Animals from ZDF along with nebivolol and ZDF along with atenolol groups presented a similar significant reduction in BP after the second month of treatment in comparison with untreated ZDF (Fig. 1a).

Biochemical parameters

At baseline, glycemia, serum triglycerides and cholesterol were significantly increased in all ZDF groups together with fasting serum insulin level, without differences between them, in comparison with control LZR, as described in Table 1. At the end of the experiment, ZDF groups presented a significant hyperglycemia compared with control LZR, but with a low fasting insulin level, which indicates the progression of the diabetic disease. Serum triglycerides and cholesterol were significantly higher in ZDF groups versus LZR. However, ZDF along with nebivolol presented a lower value when compared with untreated ZDF and ZDF along with atenolol (Table 1). No substantial differences were observed with respect to the electrolytes between the groups.

Platelet aggregation response

Platelet aggregation was significantly increased in untreated ZDF rats as compared with the other groups. Interestingly, ZDF along with atenolol and control LZR presented a similar aggregation pattern. On the contrary, ZDF along with nebivolol showed a significant lower percentage of aggregation when compared with all groups (Fig. 1b).

Echocardiographic evaluation of the left ventricle

Whereas no relevant differences between echocardiographic left ventricular dimensions as well as percentage of fractional shortening were observed in any ZDF groups or LZR at baseline, a significant increase in LVM in ZDF groups was present when compared with LZR (Table 2). At the end of the experiment, untreated ZDF as well as ZDF along with atenolol presented a significant negative modification in left ventricular dimensions together with a substantial reduction in the percentage of fractional shortening relative to control LZR (Table 2). However, ZDF with nebivolol showed a similar echocardiography pattern with actual preservation in percentage of fractional shortening, which was not different from the one observed in control LZR (Table 2). In addition, LVM was significantly increased in all ZDF groups when compared with the baseline values (Table 2). Nevertheless, ZDF along with nebivolol presented a lower and significant LVM versus untreated ZDF as well as ZDF along with atenolol (Table 2).

Organ bath studies (*in vitro*) in aortic rings

Developed tensions to Phe (10^{-8} to 10^{-4} mol/l) in aortic rings were similar in all ZDF groups as well in LZR (Fig. 1c). The mean pD2 value calculated for Phe did not present any difference between groups. Concentration–response relaxation curves were evoked by cumulative addition of ACh (10^{-8} to 10^{-4} mol/l) on aortic rings precontracted with Phe (10^{-4} mol/l). In Phe-induced contraction, endothelium-dependent relaxation to ACh was impaired significantly ($P < 0.01$) in untreated ZDF and ZDF along with atenolol aortic rings compared with ZDF along with nebivolol and control LZR (ZDF = 32.1 ± 5.5%; ZDF along with nebivolol = 86.3 ± 4.4%; ZDF along with atenolol = 44.2 ± 5.0%; and LZR = 90.1 ± 6.1%; Fig. 1d). In addition, during Phe-induced contraction, endothelium-independent relaxation to SNP was also higher in ZDF along with nebivolol and LZR in comparison with untreated ZDF and ZDF along with atenolol (ZDF = 60 ± 3.5%; ZDF along with nebivolol = 85.1 ± 3.4%; ZDF along with atenolol = 74.8 ± 3.3%; and LZR = 88.2 ± 5.9%; Fig. 1e).

Fig. 1

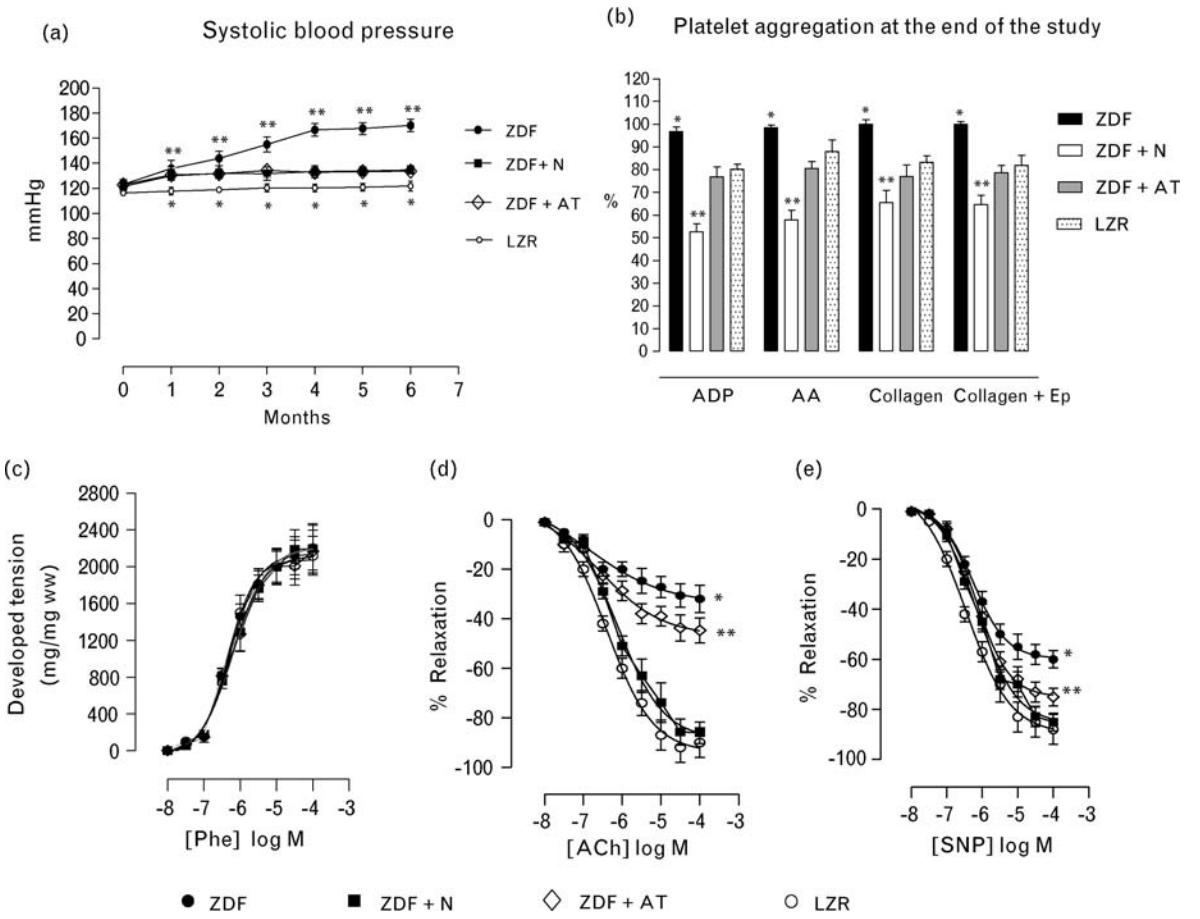

Blood pressure evaluation, platelet aggregation and vascular reactivity studies. (a) SBP evolution throughout the study. *versus all groups, $P<0.01$; **versus ZDF + N and ZDF + AT, $P<0.01$. (b) Platelet aggregation at the end of the study. *versus all groups, $P<0.01$; **versus ZDF + AT and LZR, $P<0.01$. (c), (d) and (e) Concentration–response curve to phenylephrine, acetylcholine and sodium nitroprusside in aortic rings. *versus all groups, $P<0.01$; **versus ZDF + N and LZR, $P<0.01$. AA, arachidonic acid; Ach, acetylcholine; AT, atenolol; Epi, epinephrine; LZR, lean Zucker at; N, nebivolol; Phe, phenylephrine; SNP, sodium nitroprusside; ZDF, Zucker diabetic fatty.

Table 1 Body weight and laboratory parameters

	ZDF ($n=8$)	ZDF + N ($n=8$)	ZDF + AT ($n=8$)	LZR ($n=8$)
Baseline				
Body weight (g)	410 ± 24	415 ± 19	408 ± 21	219 ± 13[a]
Glycemia (mmol/l)	14.8 ± 1.5	15.0 ± 1.4	15.1 ± 1.3	5.0 ± 0.4[a]
Triglycerides (mmol/l)	7.8 ± 1.3	7.7 ± 1.4	7.7 ± 1.3	0.5 ± 0.2[a]
Cholesterol (mmol/l)	5.3 ± 1.1	5.0 ± 1.3	5.1 ± 1.4	1.6 ± 0.4[a]
Serum insulin (ng/ml)	45.9 ± 6.1	44.3 ± 6.3	46.2 ± 5.4	5.2 ± 1.3[a]
Serum sodium (mmol/l)	146.5 ± 4.7	145.9 ± 4.9	147.0 ± 5.1	146.3 ± 4.1
Serum potassium (mmol/l)	4.3 ± 0.4	4.2 ± 0.2	4.4 ± 0.1	4.3 ± 0.3
At the end of the experiment (6 months)				
Body weight (g)	604 ± 17	599 ± 18	611 ± 14	342 ± 15[a]
Glycemia (mmol/l)	28.8 ± 6.7	23.8 ± 6.9	26.1 ± 5.1	6.0 ± 0.2[a]
Triglycerides (mmol/l)	7.6 ± 1.9	4.7 ± 1.0[b]	7.4 ± 1.5	0.4 ± 0.2[a]
Cholesterol (mmol/l)	7.2 ± 0.6	4.5 ± 0.5[b]	6.9 ± 0.9	1.7 ± 0.5[a]
Serum insulin (ng/ml)	4.5 ± 0.7	6.9 ± 0.8	4.0 ± 0.7	4.8 ± 0.4
Serum sodium (mmol/l)	147.1 ± 4.4	146.8 ± 5.1	146.5 ± 4.8	145.3 ± 4.0
Serum potassium (mmol/l)	4.5 ± 0.5	4.4 ± 0.3	4.5 ± 0.4	4.3 ± 0.4

AT, atenolol; LZR, lean Zucker rat; N, nebivolol; ZDF, Zucker diabetic fatty rat. [a] LZR versus all groups ($P<0.01$). [b] ZDF + N versus ZDF and ZDF + AT ($P<0.05$).

Table 2 Echocardiographic evaluation of the left ventricle

	ZDF ($n=8$)	ZDF + N ($n=8$)	ZDF + AT ($n=8$)	LZR ($n=8$)
Baseline				
LVDD (mm)	7.10 ± 0.2	7.23 ± 0.13	7.2 ± 0.16	6.54 ± 0.35[a]
LVSD (mm)	3.75 ± 0.18	3.73 ± 0.21	3.76 ± 0.26	3.72 ± 0.22
LVPW (mm)	1.70 ± 0.14	1.69 ± 0.10	1.68 ± 0.12	1.61 ± 0.11
IVS (mm)	1.60 ± 0.10	1.61 ± 0.09	1.62 ± 0.18	1.51 ± 0.09
FS (%)	47.30 ± 3.80	48.10 ± 3.90	47.70 ± 5.30	43.20 ± 4.30
LVM (g/BW)	0.68 ± 0.05	0.71 ± 0.03	0.69 ± 0.04	0.32 ± 0.09[b]
At the end of the experiment (6 months)				
LVDD (mm)	6.78 ± 0.27	7.90 ± 0.15[c]	6.91 ± 0.31	6.61 ± 0.11[d]
LVSD (mm)	4.66 ± 0.25	3.85 ± 0.24[d]	4.55 ± 0.37	3.75 ± 0.25[d]
LVPW (mm)	2.10 ± 0.14	1.74 ± 0.08[d]	2.02 ± 0.14	1.63 ± 0.10[d]
IVS (mm)	1.96 ± 0.12	1.66 ± 0.08[d]	1.85 ± 0.16	1.53 ± 0.05[d]
FS (%)	31.2 ± 1.9	48.3 ± 3.1[d]	34.10 ± 5.2	42.5 ± 4.80[d]
LVM (g/BW)	1.36 ± 0.08	1.19 ± 0.02[e]	1.27 ± 0.04	0.52 ± 0.06[c]

AT, atenolol; BW, body weight; FS, fractional shortening; IVS, intraventricular septum; LVDD, left ventricle end-diastolic diameter; LVM, left ventricular mass; LVPW, left ventricular posterior wall; LVSD, left ventricle end-systolic diameter; LZR, lean Zucker rat; N, nebivolol; ZDF, Zucker diabetic fatty rat. [a] LZR versus all groups ($P<0.05$). [b] LZR versus all groups ($P<0.01$). [c] LZR versus all groups ($P<0.01$). [d] ZDF + N and LZR versus ZDF and ZDF + AT ($P<0.01$). [e] ZDF + N versus ZDF and ZDF + AT ($P<0.05$).

Oxidative stress evaluation in heart homogenates

Untreated ZDF and ZDF along with atenolol rats showed a significant increase in thiobarbituric acid-reactive substances (lipoperoxidation) in heart when compared with ZDF along with nebivolol and control LZR, which presented no differences between them (Table 3). Additionally, the antioxidant enzymes, catalase and CuZnSOD, were reduced in untreated ZDF and ZDF along with atenolol, together with a remarkable decrease in reduced glutathione and in the reduced glutathione (GSH)/oxidized glutathione (GSSG) ratio in heart in comparison with ZDF along with nebivolol and control LZR (Table 3). This indicates a high level of oxidative stress in ZDF rats not controlled by atenolol therapy. Finally, GPx activity, which is involved in removing H_2O_2 using GSH, the reduced form of glutathione, was significantly elevated in untreated ZDF and ZDF along with atenolol compared with ZDF along with nebivolol and control LZR (Table 3).

Morphological findings in heart

The wall/lumen ratio in small coronary vessels was significantly greater in ZDF when compared with LZR. Both ZDF with atenolol and ZDF with nebivolol showed a significant reduction in the wall/lumen ratio in comparison with ZDF. However, ZDF with nebivolol presented a higher reduction in this ratio (Table 3). Myocardial fibrosis was increased in ZDF relative to LZR. Although the atenolol treatment partially diminished heart fibrosis, there was not a statistical difference between ZDF and ZDF with atenolol groups on this variable. On the contrary, ZDF with nebivolol showed a significant reduction in myocardial fibrosis versus ZDF (Table 3).

Table 3 Oxidative stress and histological studies at the end of the experiment

	ZDF ($n=8$)	ZDF + N ($n=8$)	ZDF + AT ($n=8$)	LZR ($n=8$)
Oxidative stress parameters in kidney homogenates at the end of the experiment (6 months)				
TBARS (nmol MDA/g protein)	303.7 ± 35.3[a]	184.7 ± 14.1	245.5 ± 20.2[b]	167.8 ± 8.9
GSH (nmol/mg protein)	14.9 ± 3.2	26.3 ± 4.1[c]	17.3 ± 2.2	30.2 ± 3.3[a]
GSH/GSSG ratio	2.7 ± 0.4	5.7 ± 0.2[c]	3.1 ± 0.5	6.5 ± 0.6[a]
Catalase (nmol/mg protein)	10.1 ± 3.5	17.8 ± 2.6[c]	12.1 ± 2.2	25.9 ± 2.9[a]
CuZnSOD (U/mg protein)	3.2 ± 0.5	6.8 ± 0.8[c]	4.0 ± 0.1	8.9 ± 1.0[a]
GPx (U/mg protein)	383.4 ± 34.9	259.9 ± 14.8[c]	355.5 ± 21.2	246.0 ± 32.8[c]
Morphological and immunohistochemistry evaluation in heart at the end of the experiment (6 months)				
Wall/lumen ratio in heart vessels	2.7 ± 0.9[e]	1.3 ± 0.6	1.8 ± 0.8[d]	1.1 ± 0.4
ECM expansion (%)/cross-section	15.1 ± 3.0[d]	3.0 ± 0.9	14.0 ± 3.3[d]	1.9 ± 1.1
$TGF\beta_1$ (percentage of positive staining/cross-section)	9.5 ± 2.2[d]	1.8 ± 0.9	8.3 ± 1.7[d]	1.1 ± 0.5
PAI-1 (percentage of positive staining/cross-section)	21.0 ± 2.9[e]	3.9 ± 1.4	16.1 ± 2.2[d]	1.5 ± 0.6
Collagen III (percentage of positive staining/cross-section)	13.1 ± 3.4[d]	3.5 ± 1.2	12.0 ± 3.1[d]	1.9 ± 1.3
Collagen I (percentage of positive staining/cross-section)	11.0 ± 2.8[d]	2.8 ± 1.0	10.0 ± 2.7[d]	1.6 ± 0.9
Morphological and immunohistochemistry evaluation in aorta at the end of the experiment (6 months)				
PAI-1 (percentage of positive staining/cross-section)	10.1 ± 2.0[g]	2.3 ± 0.7	9.6 ± 1.6[f]	1.3 ± 0.7
VCAM (percentage of positive staining/cross-section)	11.2 ± 2.6[g]	3.3 ± 1.2	8.5 ± 1.7[f]	1.4 ± 0.4
PECAM (percentage of positive staining/cross-section)	1.7 ± 0.6[g]	11.0 ± 2.0	3.9 ± 1.4[f]	13.0 ± 2.5
Collagen III (percentage of positive staining/cross-section)	13.0 ± 2.8[g]	3.0 ± 0.8	10.0 ± 3.1[f]	1.2 ± 0.3

AT, atenolol; CuZnSOD, GPx, glutathione peroxidase; CuZn superoxide dismutase; ECM, extracellular matrix; GSH, reduced glutathione; GSSG, oxidized glutathione; LZR, lean Zucker rat; MDA, malondialdehyde; N, nebivolol; PAI-1, plasminogen activator inhibitor-1; PECAM, platelet endothelial cell adhesion molecule-1; TBARS, thiobarbituric acid-reactive species; $TGF\beta_1$, transforming growth factor β_1; VCAM-1, vascular cell adhesion molecule-1; ZDF, Zucker diabetic fatty rat. [a] $P<0.01$ versus all groups. [b] $P<0.01$ versus ZDF + N and LZR. [c] $P<0.01$ versus ZDF and ZDF + AT. [d] $P<0.01$ versus ZDF + N and LZR. [e] $P<0.01$ versus all groups. [f] $P<0.01$ versus ZDF + N and LZR. [g] $P<0.01$ versus all groups.

Immunostaining in heart

Both ZDF and ZDF with atenolol animals presented a marked increase in TGFβ1 in cardiac tissue when compared with LZR. In contrast, ZDF with nebivolol showed a significant lower expression of TGFβ1 in heart versus these two groups (Fig. 2c and Table 3). A large area of positive staining for PAI-1 was observed in ZDF in comparison with LZR. The treatment with atenolol partially ameliorated PAI-1 expression in heart; however, nebivolol was significantly more effective in reducing PAI-1 in comparison with atenolol (Fig. 2d and Table 3). When compared with LZR, a remarkable amount of collagen type III and type I was observed in ZDF and ZDF with atenolol. It is worth mentioning that there were no important differences between these two groups. In contrast to this finding, animals from ZDF with nebivolol group displayed a significant lower accumulation in both types of collagen versus ZDF and ZDF with atenolol (Fig. 2e and f and Table 3).

Immunostaining in aorta

PAI-1 was markedly increased in aorta from ZDF in comparison with LZR. A partial reduction in PAI-1 expression in aorta was found in ZDF with atenolol group. However, ZDF with nebivolol presented a lower expression of PAI-1 compared with ZDF and ZDF with atenolol (Fig. 3). ZDF rats displayed a significant increase in VCAM-1 expression in aorta versus LZR. Both ZDF with atenolol and ZDF with nebivolol groups showed lower expression and less positive area staining for VCAM-1 relative to the one observed in ZDF group. Nevertheless, there was a significant difference between ZDF with atenolol and ZDF with nebivolol, in favor of the latter group (Fig. 4a and b). A small area of positive staining for PECAM-1 was observed in aorta from ZDF rats in comparison with LZR. This finding was associated with less expression of PECAM-1 by immunoblotting (Fig. 4c and d). Although ZDF with atenolol rats presented some improvement in the expression of PECAM-1 in aortic wall, the ZDF with nebivolol group showed a greater

Fig. 2

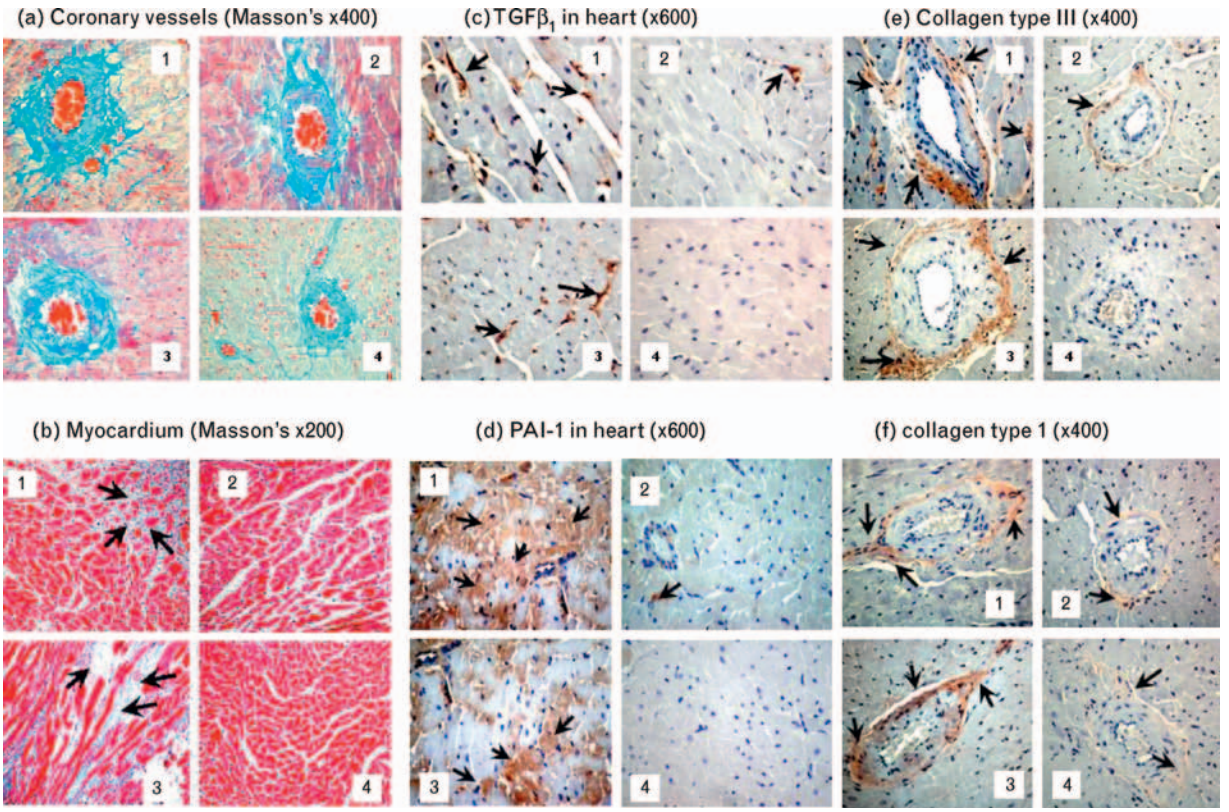

Masson's trichrome, transforming growth factor β_1, plasminogen activator inhibitor-1 and collagen in myocardium. (a) Coronary vessels (Masson's trichrome). (b) Myocardium (Masson's trichrome). Different degree of interstitial fibrosis in the myocardium in each group, as arrows indicates. (c) TGFβ_1. Arrows indicate localization of TGFβ_1 in the different groups. (d) PAI-1. Arrows indicate localization of PAI-1 in the different groups. (e) Collagen type III. Arrows indicate positive perivascular staining for collagen III in each group. (f) Collagen type I. Arrows indicate positive perivascular staining for collagen I in each group. AT, atenolol; LZR, lean Zucker rat; N, nebivolol; PAI-1, plasminogen activator inhibitor-1; TGFβ_1, transforming growth factor β_1; ZDF, Zucker diabetic fatty.

Fig. 3

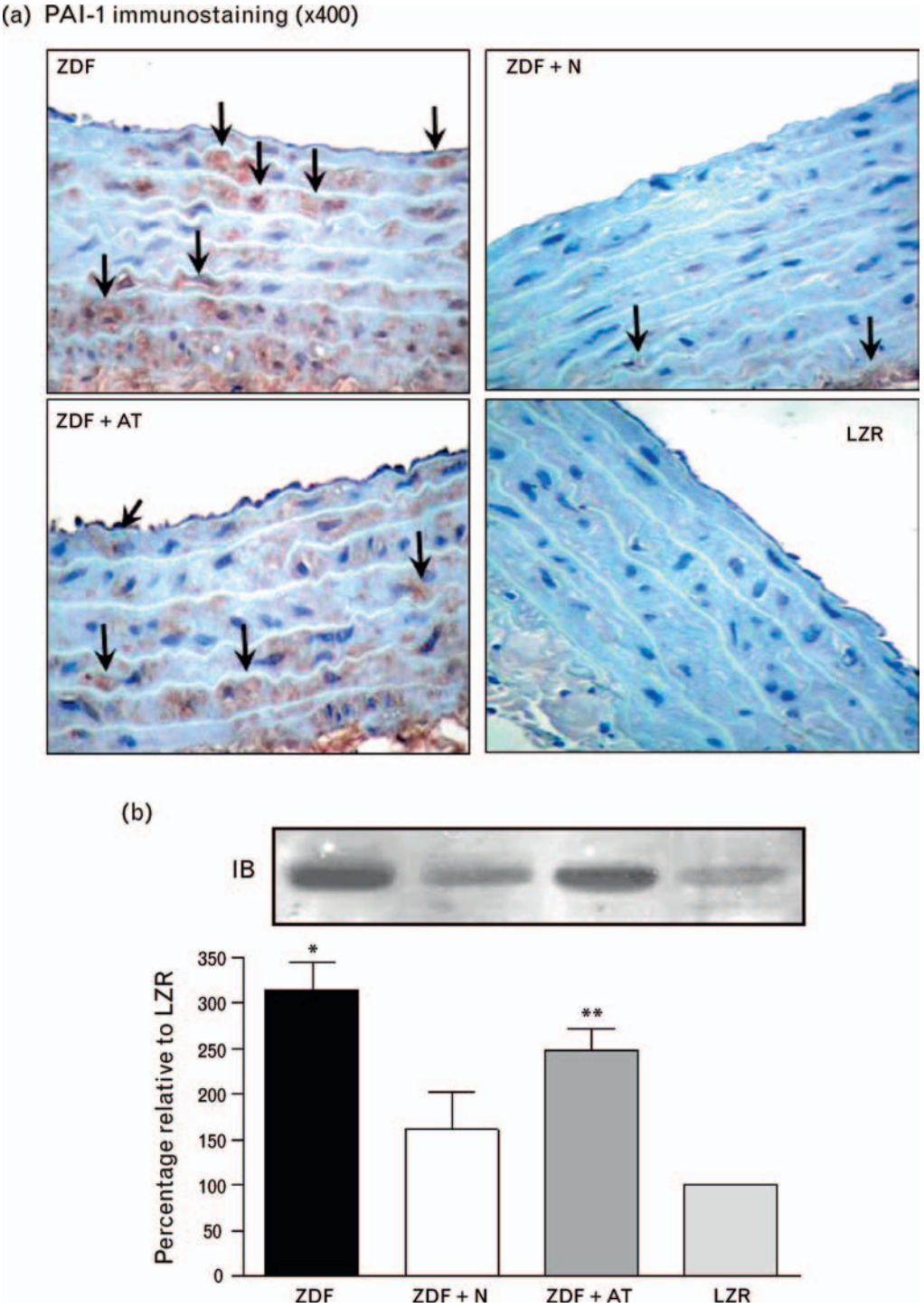

Plasminogen activator inhibitor-1 immunoexpression and localization in aorta. (a) PAI-1 immunostaining. Note a large area (arrows) in ZDF and ZDF + AT versus LZR. No major differences between ZDF + N and LZR. (b) PAI-1 protein abundance in aorta. Immunoblotting with anti-PAI-1 antibody. Scanning data are expressed as fold increase over the LZR value ± SD. $*P < 0.05$ versus LZR; $**P < 0.01$ versus LZR. AT, atenolol; LZR, lean Zucker rat; N, nebivolol; PAI-1, plasminogen activator inhibitor-1; ZDF, Zucker diabetic fatty.

Fig. 4

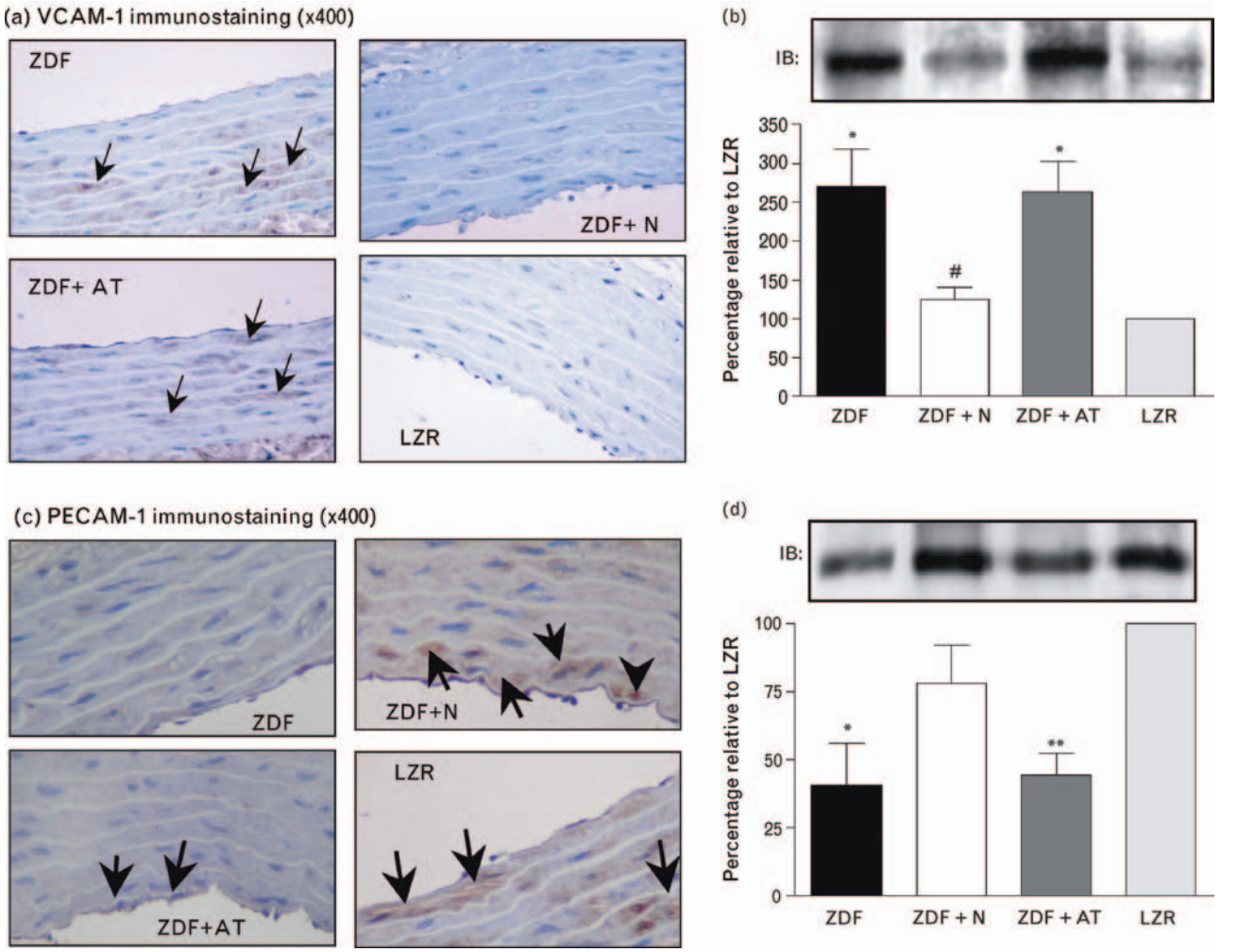

Vascular cell adhesion molecule-1 and platelet endothelial cell adhesion molecule-1 immunoexpression and localization in aorta. (a) VCAM-1 localization by immunostaining. (b) VCAM-1 protein abundance in aorta. Immunoblotting with anti-VCMA-1 antibody. (c) PECAM-1 localization by immunostaining. (d) PECAM-1 protein abundance in aorta. Immunoblotting with anti-PECAM-1 antibody. Scanning data are expressed as the fold increase over the LZR value ± SD. $^{*}P < 0.05$ versus LZR; $^{**}P < 0.01$ versus LZR; $^{\#}P < 0.05$ versus ZDF. AT, atenolol; LZR, lean Zucker rat; N, nebivolol; PECAM-1, platelet endothelial cell adhesion molecule-1; VCAM-1, vascular cell adhesion molecule-1; ZDF, Zucker diabetic fatty.

increase in PECAM-1, (Fig. 4c and d). Both ZDF and ZDF with atenolol rats presented a remarkable increase in collagen type III in aorta with respect to LZR. Even though rats from ZDF with nebivolol did not normalize the accumulation of collagen type III in aorta wall, they showed a significant reduction in collagen type III in comparison with the ZDF and ZDF with atenolol rats (Fig. 5a). ZDF rats showed a significant decrease in eNOS expression in aorta versus LZR. Both ZDF with atenolol and ZDF with nebivolol groups presented a higher expression of eNOS relative to the one observed in ZDF group. Nevertheless, there was a significant difference between ZDF with atenolol and ZDF with nebivolol, in favor of the latter group (Fig. 5b).

Discussion

In the present study, nebivolol and atenolol therapy by 6 months presented a similar reduction in BP in ZDF rats. On the contrary, despite presenting a similar blood sugar level, nebivolol displayed a better lipid profile (triglycerides and cholesterol) in comparison with atenolol.

It is well known that hyperinsulinemia, the loss of glucose-stimulated insulin secretion, and peripheral insulin resistance coexist in type 2 diabetes in human beings. In the ZDF, hyperglycemia is initially manifested at about 7 weeks of age. Then, between 7 and 10 weeks, serum insulin levels are high, but these subsequently drop, as the pancreatic β-cells stop responding to the

Fig. 5

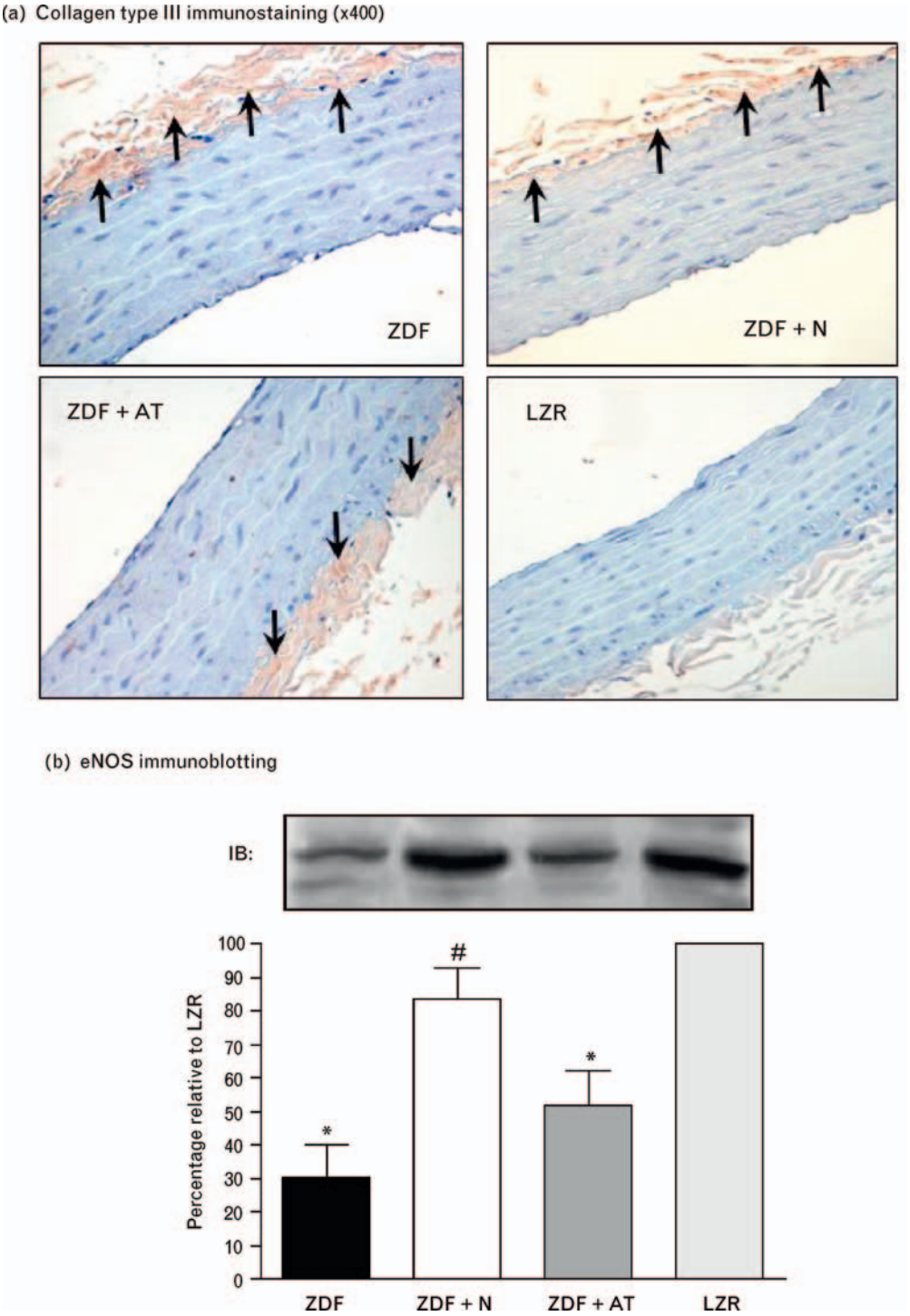

Collagen III localization by immunostaining and enhanced nitric oxide synthase protein expression in aorta. (a) Collagen III localization by immunostaining. Large area of positive staining for collagen III in ZDF and ZDF + AT with respect to LZR and ZDF + N. (b) eNOS protein abundance in aorta. Immunoblotting with anti-eNOS antibody. Scanning data are expressed as the fold increase over the LZR value ± SD. $^{*}P < 0.05$ versus LZR; $^{\#}P < 0.05$ versus ZDF. AT, atenolol; eNOS, enhanced nitric oxide synthase; LZR, lean Zucker rat; N, nebivolol; ZDF, Zucker diabetic fatty.

glucose stimulus. From the pathophysiological point of view, this loss of response to glucose is associated with the disappearance of glucose transporter (GLUT2) transporters on the β-cells in the islets. This sequence of facts was clearly appreciated in the present, which indicates the progression of diabetic state in these animals mimicking the type 2 diabetes' evolution in human beings.

Previously, in a clinical trial in which atenolol and nebivolol were compared in combination with a statin (pravastatin) to determine whether interference with lipid metabolism differed, Rizos *et al.* [24] reported that whereas atenolol considerably increased cholesterol and triglyceride levels, nebivolol decreased serum triglyceride with a favorable cholesterol profile. It is worth mentioning that persistent hypertriglyceridemia elicits a deleterious effect on the β-cell in the pancreas (lipotoxicity), and this, together with the metabolic environment of diabetes, may contribute to accelerating the negative effect on islet function. Therefore, a favorable modification in the lipid status by nebivolol may preserve the pancreatic β-cell metabolism in this scenario. Furthermore, as insulin resistance is commonly associated with endothelial dysfunction and that the exposure of vascular endothelium to high circulating levels of lipids and glucose is accompanied by reduced nitric oxide availability, the most likely mechanism that justifies the differences between nebivolol and atenolol with respect to metabolic profile is the ability of nebivolol to increase nitric oxide bioavailability, as demonstrated in animals and hypertensive patients [25].

The presence of cardiac hypertrophy deeply influences morbidity and mortality from cardiovascular diseases and is widely recognized as the most important predictor of chronic heart failure. It has been demonstrated that the cardiovascular risk of type 2 diabetes is aggravated by diabetic cardiomyopathy, leading to early left ventricular diastolic impairment or overt left ventricular dysfunction in advanced stages [26–28]. In correspondence with this statement, in our study, untreated ZDF rats presented a significant increase in LVM with a negative modification in the left ventricular dimensions by echocardiography, which was associated with a substantial reduction in the percentage of fractional shortening. The histopathology analysis of heart in this group revealed substantial morphological damage as myocardial fibrosis and high wall/lumen ratio in coronary vessels, found together with an increase in profibrotic markers such as TGFβ1 and PAI-1 and an increase in collagen types III and I accumulation. Notably, nebivolol, but not atenolol, was capable of favorably modifying these anatomic and functional alterations. The protective role of nebivolol may be justified by diverse mechanisms of action. In this sense, the antioxidative stress properties of nebivolol may be, at least in part, responsible for these effects. Accordingly, and taking into account that oxidative stress is widely recognized as a key factor in the pathogenesis of arterial hypertension, diabetes and obesity [29–33], it is not surprising that the severe lipoperoxidation observed in the heart of untreated ZDF rats, as it was indicated by the significant elevation in malondialdehyde in cardiac tissue, was controlled by nebivolol in our experiment. Furthermore, antioxidant defenses were preserved by nebivolol therapy with a reduction in oxidative parameters when compared with atenolol. Consequently, these results suggest a real profit of nebivolol against this process.

Undoubtedly, the endothelium plays an essential role in the control of local vascular tone through the production of not only vasoconstrictor and vasodilator factors but also important physiological and pathophysiological inflammatory mediators. In patients with high BP and in various experimental models of arterial hypertension, the balance between endothelium-derived relaxation factors and endothelium-derived contractile factors is altered [34,35]. Furthermore, endothelial dysfunction seems to be the trigger in atherogenesis and diabetes-associated vascular disease, and it explains, at least in part, the enhanced progression of cardiovascular disease in type 2 diabetes. In states of insulin resistance and type 2 diabetes, insulin signaling is impaired, and then, hyperglycemia leads to the increased formation of advanced glycation end-products, which quench nitric oxide, resulting in a marked decrease in nitric oxide bioavailability and the impairment of endothelial function. In our experiment, nebivolol presented a substantial endothelium-dependent and endothelium-independent relaxation in aortic rings in comparison with atenolol.

It is worth mentioning that accumulation of collagen type III in aortic wall was also diminished in the nebivolol group in comparison with that receiving atenolol therapy. Furthermore, the eNOS expression in aorta was markedly increased in the ZDF with nebivolol group.

These results are in agreement with those reported by Guerrero *et al.* [36,37], using another experimental model such as a spontaneously hypertensive rat with an equivalent dose of nebivolol for a long term. This group concluded that the antihypertensive effect of nebivolol in hypertensive rats without major metabolic alterations was accompanied by an important reduction of hypertrophy and collagen deposition, in both vessels and the left ventricle, apart from protecting endothelial function.

It is well known that the diabetic patient exhibits a pathological coagulation state, with an increased synthesis of coagulation factors and PAI-1 as well as an enhanced aggregation of platelets [38,39]. Additionally, increased vascular inflammation with an enhanced expression of VCAM-1 is observed. Nitric oxide regulates the expression of cell adhesion molecules, and increased levels of nitric oxide are associated with decreased adhesion molecule expression. Indeed, exogenous nitric oxide donors might downregulate cytokine-induced

VCAM-1 expression in cultured endothelial cells *in vitro* [40].

Another important cell adhesion molecule in vessel wall is PECAM-1, which is involved in the transduction cascade that translates the mechanical stimulation of endothelial cells into the activation of eNOS [41]. Therefore, unquestionably, a therapeutic approach that adequately modulates this particular topic acquires importance.

In the present study, the evaluation in aorta indicated that adhesion molecules, such as VCAM-1 and PECAM-1, were both favorably modified with nebivolol in the vascular wall in ZDF rats, which suggests an actual benefit of nebivolol in a prothrombosis state, as it occurs in metabolic syndrome.

It has been documented that some β-blockers, such propanolol, nebivolol and also carvedilol, are potent inhibitors of platelet function. This inhibitory effect is independent of their ability to antagonize β-receptors and may be the result of their membrane-stabilizing action [42,43]. Importantly, in our study, nebivolol presented a significant reduction in platelet aggregation in comparison with atenolol. Accordingly, in an in-vitro study [44], in which nebivolol was compared with propanolol and carvedilol, the antiaggregatory effect of nebivolol was more potent than that of the other β-blockers. This favorable action was associated with its recognized property of facilitating nitric oxide production.

This positive effect observed in our experiment may contribute to improve rheology and microcirculation, reducing thrombotic risk in a particular complex scenario such as the metabolic syndrome.

As final remarks, we may conclude that the data presented in the current study provide substantial evidence supporting an actual protective role of nebivolol in comparison with atenolol in cardiovascular tissue in a recognized animal model of metabolic syndrome, which is characterized by multiple cardiovascular risk factors.

Acknowledgements

J.E.T. and F.P.D. are career investigators from Consejo Nacional de Investigaciones Científicas y Tecnológicas of Argentina (CONICET) and received grant support from the University of Buenos Aires (UBA), CONICET and Agencia Nacional de Promoción Científica y Tecnológica of Argentina. M.C.M. is a research fellow from CONICET, and J.F.G. is a research fellow from UBA.

There are no conflicts of interest.

References

1 Cameron AJ, Shaw JE, Zimmet PZ. The metabolic syndrome: prevalence in worldwide populations. *Endocrinol Metab Clin N Am* 2004; **33**:351–375.

2 Reaven G. The metabolic syndrome or the insulin resistant syndrome? Different names, different concepts, and different goals. *Endocrinol Metab Clin N Am* 2004; **33**:283–303.

3 He J, Ogden LG, Bazzano LA, Vupputuri S, Loria C, Whelton PK. Risk factors for congestive heart failure in US men and women: NHANES I epidemiologic follow-up study. *Arch Intern Med* 2001; **161**:996–1002.

4 Fox CS, Larson MG, Leip EP, Meigs JB, Wilson PW, Levy D. Glycemic status and development of kidney disease: the Framingham Heart Study. *Diabetes Care* 2005; **28**:2436–2440.

5 Malik S, Wong ND, Franklin SS, Kamath TV, L'Italien GJ, Pio JR, Williams GR. Impact of the metabolic syndrome on mortality from coronary heart disease, cardiovascular disease and all cause in United States adults. *Circulation* 2004; **110**:1245–1250.

6 Masuo K, Kawaguchi H, Mikami H, Ogihara T, Tuck ML. Serum uric acid and plasma norepinephrine concentrations predict subsequent weight gain and blood pressure elevation. *Hypertension* 2003; **42**:474–480.

7 Berne C, Fagius J, Pollare T, Hjemdahl P. The sympathetic response to euglycaemic hyperinsulinaemia: evidence from microelectrode nerve recordings in healthy subjects. *Diabetologia* 1992; **35**:873–879.

8 Eikelis N, Schlaich M, Aggarwal A, Kaye D, Esler M. Interactions between leptin and the human sympathetic nervous system. *Hypertension* 2003; **41**:1072–1079.

9 Benthem L, Kuipers F, Steffens AB, Scheurink AJW. Excessive portal venous supply of long-chain free fatty acids to the liver, leading to hypothalamus-pituitary-adrenalaxis and sympathetic activation as a key to the development of syndrome X. *Ann N Y Acad Sci* 1999; **892**:308–311.

10 Bray GA. The Zucker-fatty rat: a review. *Fed Proc* 1977; **36**:148–153.

11 Kava R, Greenwood MR, Johnson PR. Zucker (fa/fa) rats. *ILAR News* 1990; **32**:4–8.

12 Kurtz TW, Morris RC, Pershadsingh HA. The Zucker fatty rat as a genetic model of obesity and hypertension. *Hypertension* 1989; **13**:896–901.

13 Toblli JE, Cao G, Casas G, Mazza ON. In vivo and in vitro effects of nebivolol on penile structures in hypertensive rats. *Am J Hypertens* 2006; **19**:1226–1232.

14 Toblli J, Stella I, Néstor Mazza O, Ferder L, Inserra F. Protection of cavernous tissue in male spontaneously hypertensive rats. Beyond blood pressure control. *Am J Hypertens* 2004; **17**:516–522.

15 Carusio N, Wangensteen R, Filippelli A, Andriantsitohaina R. Oral administration of polyphenolic compounds from cognac decreases ADP-induced platelet aggregation and reduces chronotropic effect of isoprenaline in rats. *Physiol Res* 2008; **57**:517–524.

16 Chance B, Maehly A. Assay of catalase and peroxidase. In: Colowick SP, Kaplan NO, editors. *Methods in enzymology, Vol. 2*. New York: Academic Press; 1955. pp. 764–768.

17 Paoletti F, Aldinucci D, Mocall A, Caparrini A. A sensitive spectrophotometric method for the determination of superoxide dismutase activity in tissue extracts. *Anal Biochem* 1986; **154**:536–541.

18 Niehaus W, Samuelson B. Formation of malondialdehyde from phospholipids arachidonate during microsomal lipid peroxidation. *Eur J Biochem* 1968; **6**:126–130.

19 Lowry O, Rosebrough N, Farr A, Randall R. Protein measurement with the Folin-phenol reagent. *J Biol Chem* 1954; **193**:265–275.

20 Toblli JE, DeRosa G, Rivas C, Cao G, Piorno P, Pagano P, Forcada P. Cardiovascular protective role of a low-dose antihypertensive combination in obese Zucker rats. *J Hypertens* 2003; **21**:611–620.

21 Kovanecz I, Nolazco G, Ferrini MG, Toblli JE, Heydarkhan S, Vernet D, *et al.* Early onset of fibrosis within the arterial media in a rat model of type 2 diabetes mellitus with erectile dysfunction. *BJU Int* 2009; **103**:1396–1404.

22 Giani JF, Gironacci MM, Muñoz MC, Peña C, Turyn D, Dominici FP. Angiotensin-(1-7) stimulates the phosphorylation of JAK2, IRS-1 and Akt in rat heart in vivo: role of the AT1 and Mas receptors. *Am J Physiol Heart Circ Physiol* 2007; **293**:H1154–H1163.

23 Muñoz MC, Argentino DP, Dominici FP, Turyn D, Toblli JE. Irbersartan restores the in vivo insulin signaling pathway leading to Akt activation in obese Zucker rats. *J Hypertens* 2006; **24**:1607–1617.

24 Rizos E, Bairaktari E, Kostoula A, Hasiotis G, Achimastos A, Ganotakis E, *et al.* The combination of nebivolol plus pravastatin is associated with a more beneficial metabolic profile compared to that of atenolol plus pravastatin in hypertensive patients with dyslipidemia: a pilot study. *J Cardiovasc Pharmacol Ther* 2003; **8**:127–134.

25 Agabiti Rosei E, Rizzoni D. Metabolic profile of nebivolol, a beta-adrenoceptor antagonist with unique characteristics. *Drugs* 2007; **67**:1097–1107.

26 Fein FS, Sonnenblick EH. Diabetic cardiomyopathy. *Cardiovasc Drugs Ther* 1994; **8**:65–73.

27 Picano E. Diabetic cardiomyopathy. The importance of being earliest. *J Am Coll Cardiol* 2003; **42**:454–457.

28 El-Omar MM, Yang ZK, Phillips AO, Shah AM. Cardiac dysfunction in the Goto-Kakizaki rat. A model of type II diabetes mellitus. *Basic Res Cardiol* 2004; **99**:133–141.

29 Evans JL, Goldfine ID, Maddux BA, Grodsky GM. Oxidative stress and stress-activated signaling pathways: a unifying hypothesis of type 2 diabetes. *Endocr Rev* 2002; **23**:599–622.

30 Dhalla NS, Temsah RM, Netticadan T. Role of oxidative stress in cardiovascular diseases. *J Hypertens* 2000; **18**:655–673.

31 Schnackenberg CG, Wilcox CS. Two-week administration of tempol attenuates both hypertension and renal excretion of 8-iso prostaglandin F2α. *Hypertension* 1999; **33**:424–428.

32 Chen YF, Cowley AW, Zou AP. Increased H2O2 counters the vasodilator and natriuretic effects of superoxide dismutation by tempol in renal medulla. *Am J Physiol* 2003; **285**:R827–R833.

33 Charloux C, Paul M, Loisance D, Astier A. Inhibition of hydroxyl radical produced by lactobionate, adenine, and tempol. *Free Radic Biol Med* 1995; **19**:669–704.

34 Lüscher TF, Vanhoutte PM. Endothelium-dependent contractions to acetylcholine in the aorta of the spontaneously hypertensive rat. *Hypertension* 1986; **8**:344–348.

35 Tschudi M, Mesaros S, Lüscher T, Malinski T, *et al.* Direct in situ measurement of nitric oxide in mesenteric resistance arteries. Increased decomposition by superoxide in hypertension. *Hypertension* 1996; **27**:32–35.

36 Guerrero El, Ardanaz N, Sevilla MA, Arévalo MA, Montero MJ. Cardiovascular effects of nebivolol in spontaneously hypertensive rats persist after treatment withdrawal. *J Hypertens* 2006; **24**:151–158.

37 Guerrero E, Voces F, Ardanaz N, Montero MJ, Arévalo M, Sevilla MA. Long-term treatment with nebivolol improves arterial reactivity and reduces ventricular hypertrophy in spontaneously hypertensive rats. *J Cardiovasc Pharmacol* 2003; **42**:348–355.

38 Ogawa H, Nakayama M, Morimoto T, Uemura S, Kanauchi M, Doi N, *et al.* Japanese Primary Prevention of Atherosclerosis With Aspirin for Diabetes (JPAD) Trial Investigators. Low-dose aspirin for primary prevention of atherosclerotic events in patients with type 2 diabetes: a randomized controlled trial. *JAMA* 2008; **300**:1234–1241.

39 Nicolucci A. Aspirin for primary prevention of cardiovascular events in diabetes: still in open question. *JAMA* 2008; **300**:2180–2181.

40 Khan BV, Harrison DG, Olbrych MT, Alexander RW, Medford RM. Nitric oxide regulates vascular cell adhesion molecule 1 gene expression and redox-sensitive transcriptional events in human vascular endothelial cells. *Proc Natl Acad Sci U S A* 1996; **93**:9114–9119.

41 Fleming I, Fisslthaler B, Dixit M, Busse R. Role of PECAM-1 in the shear-stress-induced activation of Akt and the endothelial nitric oxide synthase (eNOS) in endothelial cells. *J Cell Sci* 2005; **118**:4103–4111.

42 Weksler BB, Gillick M, Pink J. Effect of propranolol on platelet function. *Blood* 1977; **49**:185–196.

43 Kerry R, Scrutton MC, Wallis RB. Beta-adrenoceptor antagonists and human platelets: relationship of effects to lipid solubility. *Biochem Pharmacol* 1984; **33**:2615–2622.

44 Falciani M, Rinaldi B, D'Agostino B, Mazzeo F, Rossi S, Nobili B, *et al.* Effects of nebivolol on human platelet aggregation. *J Cardiovasc Pharmacol* 2001; **38**:922–929.